

Properties of Ca^{2+} Transport in Mitochondria of *Drosophila melanogaster**^[5]

Received for publication, June 9, 2011, and in revised form, September 1, 2011. Published, JBC Papers in Press, October 7, 2011, DOI 10.1074/jbc.M111.268375

Sophia von Stockum^{†1}, Emy Basso[‡], Valeria Petronilli[‡], Patrizia Sabatelli[§], Michael A. Forte[¶], and Paolo Bernardi^{‡#2}

From the [†]Consiglio Nazionale delle Ricerche Institute of Neuroscience and Department of Biomedical Sciences, University of I-35121 Padova, Italy and [§]Institute of Molecular Genetics at the Istituto Ortopedico Rizzoli, I-40126 Bologna, Italy, and the [¶]Vollum Institute, Oregon Health & Sciences University, Portland, Oregon 97239

Background: We have studied the properties of Ca^{2+} transport in *Drosophila* mitochondria.

Results: *Drosophila* mitochondria possess Ca^{2+} transport systems matching their mammalian equivalents but have a unique selective Ca^{2+} release channel that does not mediate swelling.

Conclusion: The *Drosophila* Ca^{2+} release channel is involved in Ca^{2+} homeostasis rather than cell death.

Significance: This channel may represent the missing link between the permeability transition pore of yeast and mammals.

We have studied the pathways for Ca^{2+} transport in mitochondria of the fruit fly *Drosophila melanogaster*. We demonstrate the presence of ruthenium red (RR)-sensitive Ca^{2+} uptake, of RR-insensitive Ca^{2+} release, and of Na^{+} -stimulated Ca^{2+} release in energized mitochondria, which match well characterized Ca^{2+} transport pathways of mammalian mitochondria. Following larger matrix Ca^{2+} loading *Drosophila* mitochondria underwent spontaneous RR-insensitive Ca^{2+} release, an event that in mammals is due to opening of the permeability transition pore (PTP). Like the PTP of mammals, *Drosophila* Ca^{2+} -induced Ca^{2+} release could be triggered by uncoupler, diamide, and *N*-ethylmaleimide, indicating the existence of regulatory voltage- and redox-sensitive sites and was inhibited by tetracaine. Unlike PTP-mediated Ca^{2+} release in mammals, however, it was (i) insensitive to cyclosporin A, ubiquinone 0, and ADP; (ii) inhibited by P_i , as is the PTP of yeast mitochondria; and (iii) not accompanied by matrix swelling and cytochrome *c* release even in KCl-based medium. We conclude that *Drosophila* mitochondria possess a selective Ca^{2+} release channel with features intermediate between the PTP of yeast and mammals.

Mitochondria play a pivotal role in cellular Ca^{2+} homeostasis and thereby participate in the orchestration of a diverse range of cellular activities. Indeed, the mitochondrial proton electrochemical gradient is used not only to synthesize ATP but also to accumulate cations into the mitochondrial matrix (1–4). Consequently, when local cytoplasmic free Ca^{2+} levels rise, mitochondria rapidly accumulate cytoplasmic Ca^{2+} and then grad-

ually release it as normal cytoplasmic levels are restored, amplifying and sustaining signals arising from elevation of cytoplasmic Ca^{2+} , as well as protecting cells and neurons against transient elevation in intracellular Ca^{2+} during periods of hyperactivity (1, 5, 6). As a result, the mechanisms controlling cellular and mitochondrial Ca^{2+} homeostasis, metabolism, and bioenergetics must function as a tightly integrated system within the overall cellular Ca^{2+} homeostatic network (2, 7–9).

The pathways responsible for mitochondrial Ca^{2+} uptake and release have been intensely studied on a functional level for >50 years. In energized mitochondria, the Ca^{2+} uniporter mediates Ca^{2+} uptake across the inner mitochondrial membrane, whereas exchangers (Ca^{2+} for Na^{+} and/or H^{+}) are responsible for Ca^{2+} efflux (9–13). However, when the mitochondrial Ca^{2+} load exceeds the capacity of inner membrane exchangers, an additional pathway for Ca^{2+} efflux from mitochondria may exist through opening of the permeability transition pore (PTP).³

The mitochondrial permeability transition (PT) describes a process of Ca^{2+} -dependent, tightly regulated increase in the permeability of the inner mitochondrial membrane due to the opening of a high-conductance channel, the PTP (10). PTP opening causes collapse of the mitochondrial membrane potential ($\Delta\psi$) and Ca^{2+} release through the pore itself, an event that for short “open” times may indeed be involved in physiological Ca^{2+} homeostasis (14, 15), as recently shown in mouse hearts (16) and adult neurons (17) consistent with a role of the PTP in cell signaling (18). Prolonged opening of the PTP, on the other hand, causes stable depolarization, loss of ionic homeostasis, depletion of pyridine nucleotides, respiratory inhibition, matrix swelling, release of cytochrome *c*, and cell death via apoptosis or necrosis depending on a variety of additional factors, among which cellular ATP and Ca^{2+} levels play a major role (19).

* This work was supported, in whole or in part, by National Institutes of Health Grant GM069883. This work was also supported in part by grants from the Fondazione Cariparo and the University of Padova Progetti di Eccellenza Models of Mitochondrial Diseases.

^[5] The on-line version of this article (available at <http://www.jbc.org>) contains supplemental Figs. 1–3.

¹ This work was submitted to partially fulfill the requirements for a PhD in Cell Biology at the University of Padova.

² To whom correspondence should be addressed: Dept. of Biomedical Sciences, University of Padova, Viale Giuseppe Colombo 3, I-35121 Padova, Italy. Fax: 39-049-827-6361; E-mail: bernardi@bio.unipd.it.

³ The abbreviations used are: PTP, permeability transition pore; CRC, Ca^{2+} retention capacity; $\Delta\psi$, inner membrane potential difference; FCCP, carbonylcyanide-*p*-trifluoromethoxyphenylhydrazone; NEM, *N*-ethylmaleimide; OMM, outer mitochondrial membrane; RR, ruthenium red; TMRM, tetramethylrhodamine methyl ester.

Mitochondrial Ca^{2+} Transport in *Drosophila*

Together with matrix Ca^{2+} , P_i is an essential inducer of PTP opening in mammals (19), whereas P_i exerts an inhibitory action on the yeast permeability pathways triggered by ATP and energization (20–24; see Ref. 25 for a recent review). In mammals, the PTP can be desensitized by submicromolar concentrations of the immunosuppressant drug cyclosporin A (26–28) via an interaction with its matrix receptor cyclophilin D (29). Our recent discovery that the inhibitory effect of cyclosporin A and of cyclophilin D ablation on the pore requires P_i (30) opens new scenarios. Indeed, this observation may bridge the gap between the pore of yeast and mammals, which we have hypothesized to be much closer than previously thought (31; see Ref. 32 for a review of earlier literature).

Despite its importance as a model organism, the characteristics of mitochondrial Ca^{2+} transport have been little studied in *Drosophila melanogaster*. The present study demonstrates that *Drosophila* mitochondria possess Ca^{2+} transport systems that are very close to those of mammals and that they can undergo a ruthenium red (RR)-insensitive Ca^{2+} -induced Ca^{2+} release through a selective channel that is insensitive to cyclosporin A and inhibited by P_i , and whose general features may be intermediate between the properties of the PTP of yeast and that of mammals.

EXPERIMENTAL PROCEDURES

Cell Cultures— S_2R^+ cells (33) were cultured in Schneider's insect medium supplemented with 10% heat-inactivated FBS and kept in 75-cm² T flasks or in tissue culture dishes (245 × 245 × 25 mm) at 25 °C.

Cell Permeabilization—Cells were detached with a sterile cell scraper, centrifuged at 200 × *g* for 10 min, and washed twice with Dulbecco's PBS without Ca^{2+} and Mg^{2+} , pH 7.4 (Euroclone). The resulting pellet was resuspended in 130 mM KCl, 10 mM MOPS-Tris, pH 7.4 (KCl medium), containing 150 μM digitonin and 1 mM EGTA-Tris and incubated for 20 min on ice (6 × 10⁷ cells × ml⁻¹). Cells were then diluted 1:5 in KCl medium containing 10 μM EGTA-Tris and centrifuged at 200 × *g* in a refrigerated centrifuge (4 °C) for 6 min. The final pellet was resuspended in KCl medium containing 10 μM EGTA-Tris at 4 × 10⁸ cells × ml⁻¹ and kept on ice.

Fluorescent Staining of S_2R^+ Cell Mitochondria—In the experiments of Fig. 1A energization of mitochondria in both intact and permeabilized S_2R^+ cells was analyzed based on accumulation of the potentiometric probe tetramethyl rhodamine methyl ester (TMRM, Molecular Probes). Three days before the experiments, cells were seeded onto sterilized 24-mm round glass coverslips at 2 × 10⁶ cells per well in 2 ml of Schneider's medium supplemented with 10% FBS. On the day of experiment, cells were washed once with PBS and incubated for 20 min at room temperature with 1 ml of serum-free Schneider's medium supplemented with 1 μg/ml cyclosporin H and 10 nM TMRM. Cyclosporin H is an inhibitor of the plasma membrane multidrug resistance pumps and allows an appropriate loading with the probe by preventing its extrusion at the plasma membrane (34). Images were acquired with an Olympus IX71/IX51 inverted microscope equipped with a xenon light source (75 watts) for epifluorescence illumination and with a

12-bit digital cooled CCD camera (Micromax). For detection of TMRM fluorescence, 568 ± 25-nm bandpass excitation and 585-nm long pass emission filter settings were used.

In the experiments of Fig. 1C, mitochondrial membrane potential was measured using a Perkin-Elmer LS50B spectrofluorometer and evaluated based on the fluorescence quenching of Rhodamine 123. Two milliliters of 130 mM KCl, 10 mM MOPS-Tris, 5 mM Pi-Tris, 10 μM EGTA, 0.15 μM Rhodamine 123, pH 7.4, were added to the cuvette. The fluorescence of Rhodamine 123 was monitored at the excitation and emission wavelengths of 503 and 523 nm, respectively, with the slit width set at 2.5 nm. After a short incubation to reach stabilization of the signal, 2 × 10⁷ permeabilized S_2R^+ cells were added to the cuvette. Further additions were as indicated in the figure legends.

Electron Microscopy— S_2R^+ cells were washed with PBS and fixed in 2.5% glutaraldehyde in 0.1 M potassium phosphate buffer, pH 7.4, for 2 h at 4 °C. After washing with 0.15 M potassium phosphate buffer, pH 7.0, cells were finally embedded in 2% gelatin as described previously (35). Gelatin-embedded samples were post-fixed with 1% osmium tetroxide in cacodylate buffer 0.1 M, pH 7.4, and embedded in Epon812 resin, sectioned, and stained following standard procedures (36). Ultra-thin sections were observed with a Philips EM400 transmission electron microscope operating at 100 kV.

Mitochondrial Respiration—Rates of mitochondrial respiration were measured using a Clark-type oxygen electrode equipped with magnetic stirring and thermostatic control maintained at 25 °C, and additions were made through a syringe port in the frosted glass stopper sealing the chamber. Intact S_2R^+ cells were incubated in Hank's balanced salt solution supplemented with 10 mM glucose and 5 mM P_i -Tris, pH 7.4, whereas digitonin-permeabilized cells (see above) were incubated in 130 mM KCl, 10 mM MOPS-Tris, 5 mM P_i -Tris, 5 mM succinate-Tris, 10 μM EGTA, pH 7.4. In both cases, 2 × 10⁷ cells in 2 ml were used, and further additions are specified in the figure legends.

Light Scattering and Mitochondrial Ca^{2+} Fluxes—Light scattering at 90° was monitored with a PerkinElmer LS50B spectrofluorimeter at 540 nm with a 5.5-nm slit width. Extramitochondrial Ca^{2+} was measured with Calcium Green 5N (Molecular Probes) using either the PerkinElmer LS50B spectrofluorometer equipped with magnetic stirring (excitation and emission wavelengths of 505 and 535 nm, respectively) or a Fluoroskan Ascent FL (Thermo Electron Corp.) equipped with a plate shaker (excitation and emission wavelengths of 485 and 538 nm, respectively with a 10-nm band pass filter). The incubation medium contained 130 mM KCl, 10 mM MOPS-Tris, 5 mM succinate-Tris, 10 μM EGTA, 2 μM rotenone, pH 7.4, and P_i -Tris as indicated in the figure legends. In the Ca^{2+} measurements, 0.5 μM Calcium-Green 5N was also added. Permeabilized cells (2 × 10⁷ in a final volume of 2 ml in the PerkinElmer spectrofluorometer and 2 × 10⁶ in a final volume of 0.2 ml in the Fluoroskan) were used. Further additions were made as indicated in the figure legends.

Western Blotting—Cell suspensions were centrifuged at 3000 × *g* at 4 °C. Proteins from the supernatants were precipitated in acetone at -20 °C and centrifuged for 30 min at

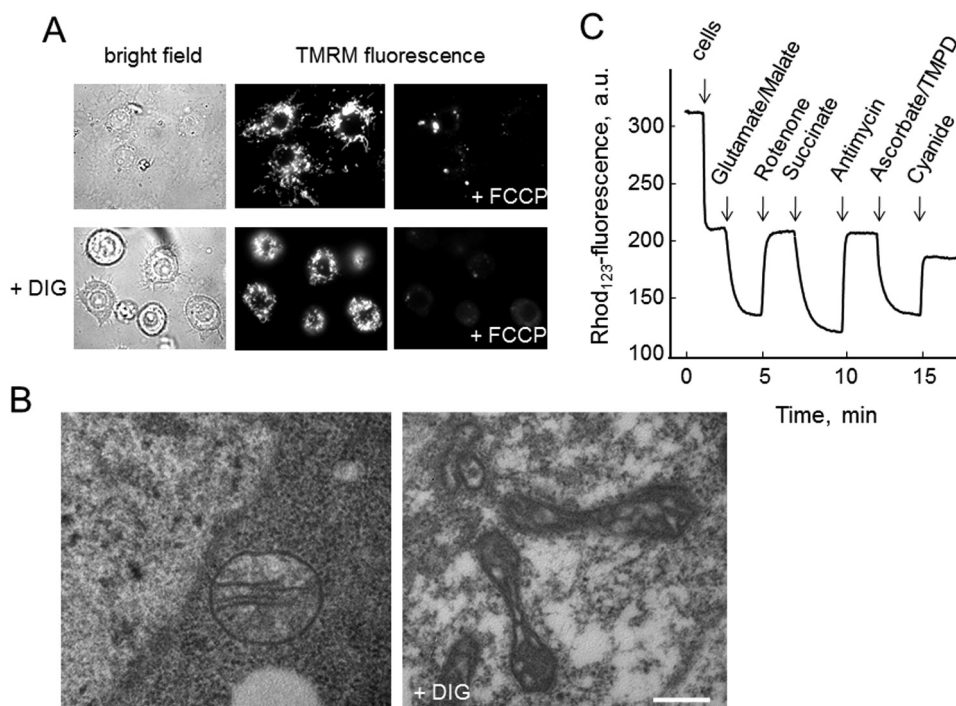


FIGURE 1. **Evaluation of mitochondrial energization and membrane potential in intact and permeabilized *Drosophila* S_2R^+ cells.** *A*, cells were seeded on glass coverslips, loaded with 10 nM TMRM as described under "Experimental Procedures," and observed under bright field conditions or for TMRM fluorescence before and after the addition of 4 μM FCCP either without further additions (*upper row*) or after permeabilization with 30 μM digitonin (+DIG, *lower row*). *B*, ultrastructural analysis of untreated (*left panel*) and digitonin-permeabilized (*right panel*, DIG) S_2R^+ cells; bar, 300 nm for both panels. *C*, cells were digitonized as described under "Experimental Procedures" and incubated in 130 mM KCl, 10 mM MOPS-Tris, 10 μM EGTA, and 0.15 μM Rhodamine 123 (Rhod_{123}), pH 7.4. Further additions were 5 mM glutamate-Tris plus 2.5 mM malate-Tris, 2 μM rotenone, 5 mM succinate-Tris, 0.1 $\mu\text{g/ml}$ antimycin A, 5 mM ascorbate-Tris plus 100 μM tetramethyl-*p*-phenylene diamine (TMPD) and 2 mM KCN. *a.u.*, arbitrary units.

18,000 $\times g$ at 4 °C. Pellets were washed twice in 20% methanol and finally solubilized in Laemmli gel sample buffer. Cell pellets were lysed in a buffer containing 150 mM NaCl, 20 mM Tris, pH 7.4, 5 mM EDTA-Tris, 10% glycerol, 1% Triton X-100, and supplemented with protease and phosphatase inhibitor cocktails (Sigma), and kept on ice for 20 min. Suspensions were then centrifuged at 18,000 $\times g$ for 25 min at 4 °C to remove insoluble materials. The supernatants were solubilized in Laemmli gel sample buffer. Samples were separated by 15% SDS-PAGE and transferred electrophoretically to nitrocellulose membranes using a Mini Trans-Blot system (Bio-Rad). Western blotting was performed in PBS containing 3% nonfat dry milk with monoclonal mouse anti-cytochrome *c* (BD Biosciences), monoclonal mouse anti-OxPhos complex IV subunit I (Invitrogen), or rabbit polyclonal anti-TOM20 (Santa Cruz Biotechnology) antibodies.

Reagents and Statistics—All chemicals were of the highest purity commercially available. Reported results are typical of at least three replicates for each condition, and error bars refer to the S.D.

RESULTS

We initially isolated mitochondria from *Drosophila* flight muscles after dissection of the thoraces to prevent contamination from the yeast on which *Drosophila* feeds and that may be present in the abdomen. Despite our great efforts mitochondria were of poor quality, as judged from the respiratory control ratios (results not shown). An additional problem we encountered was that the low yield of these preparations did not allow

a reproducible analysis of the Ca^{2+} transport properties of mitochondria. Thus, we characterized mitochondrial function in intact S_2R^+ *Drosophila* cells and then used digitonin permeabilization to access mitochondria *in situ*, an approach that we have successfully applied to mammalian cells (37) and to cells from 6-h-old embryos from *Danio rerio* (zebrafish) (38).

Mitochondria in both intact and permeabilized S_2R^+ cells were energized, as shown by fluorescence images after the addition of the potentiometric probe TMRM (Fig. 1A). Mitochondria appeared as bright bodies, and fluorescence was lost upon addition of an uncoupler (Fig. 1A). Ultrastructural analysis of intact S_2R^+ cells revealed round-shaped mitochondria with thin cristae aligned in parallel rows (Fig. 1B, *left panel* illustrates a typical example), which is strikingly similar to the morphology of mammalian mitochondria *in situ* and to the "orthodox" configuration of Hackenbrock (39). After digitonin treatment, most cells showed evidence of permeabilization as reflected by a change in the electron density of the cytoplasm and loss of chromatin definition (results not shown), but the overall morphology of organelles was retained (Fig. 1B, *right panel*). Mitochondria, however, now displayed a "condensed" configuration very similar to that of isolated mammalian mitochondria (39), which is characterized by an electron-dense matrix and evident and well preserved cristae and outer membrane (Fig. 1B, *right panel*).

Digitonin-permeabilized cells are accessible to substrates, and this allows the study of their response to energization. Mitochondria readily developed a membrane potential (as

Mitochondrial Ca²⁺ Transport in *Drosophila*

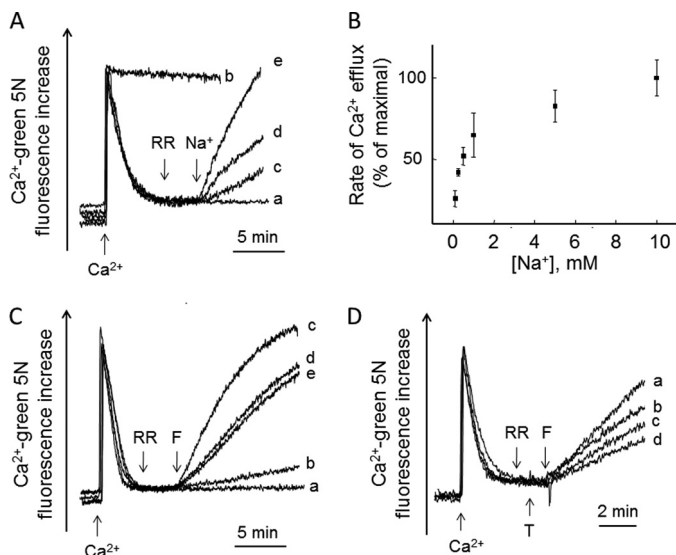


FIGURE 2. Mitochondrial Ca²⁺ transport in permeabilized *Drosophila* S₂R⁺ cells. Digitonin-permeabilized S₂R⁺ cells were incubated in 130 mM KCl, 10 mM MOPS-Tris, 5 mM P_i-Tris, 5 mM succinate-Tris, 10 μM EGTA, 2 μM rotenone, and 0.5 μM Calcium Green 5N, pH 7.4. *A*, in trace *b* only, the incubation medium was supplemented with 0.2 μM RR; where indicated, 25 μM Ca²⁺ with no further additions (trace *a*) or followed by 0.2 μM RR and by 0.1 mM (trace *c*), 1 mM (trace *d*), or 10 mM NaCl (trace *e*). *B*, rate of Na⁺-induced Ca²⁺ release obtained in protocols such as those depicted in *A* as a function of the added Na⁺ concentration; values were normalized to the rate observed after the addition of 10 mM NaCl (taken as maximal), and error bars report the S.D. of triplicate experiments. *C*, in trace *e* only, the medium was supplemented with 1 μg/ml cyclosporin A; where indicated, 25 μM Ca²⁺ was added followed by the addition of 0.2 μM RR and/or 0.5 μM FCCP where indicated by arrows as follows: no addition after the Ca²⁺ pulse (*a*), RR only (*b*), FCCP only (*c*), and RR and FCCP (*d* and *e*). *D*, where indicated, 25 μM Ca²⁺ pulse, 0.2 μM RR, 0.5 mM (*b*), 1 mM (*c*), or 2 mM (*d*) tetracaine and 0.5 μM FCCP. Trace *a* was obtained after the addition of RR and FCCP without tetracaine.

judged on the basis of fluorescence quenching of Rhodamine 123 upon addition of the complex I substrates glutamate and malate (Fig. 1C). The sequential addition of rotenone, succinate, antimycin A, ascorbate plus tetramethyl-*p*-phenylene diamine, and finally cyanide caused the expected repolarization-depolarization cycles that indicate functioning of all respiratory complexes (Fig. 1C).

Intact S₂R⁺ cells displayed a good respiratory activity that was largely inhibited by oligomycin, indicating that a prevalent fraction of oxygen uptake was devoted to ATP synthesis. Basal respiration could be stimulated >5-fold by the addition of the uncoupler carbonyl cyanide *p*-trifluoromethoxyphenylhydrazone (FCCP), indicating a good reserve capacity of the respiratory chain (supplemental Fig. 1A). In addition, permeabilized cells displayed a good phosphorylation capacity after energization with succinate (supplemental Fig. 1B), and we used these conditions to study the properties of mitochondrial Ca²⁺ transport.

Energized mitochondria readily took up and retained a Ca²⁺ pulse of 25 μM (Fig. 2A, trace *a*), in a process that was fully inhibited by pretreatment with RR (Fig. 2A, trace *b*), the inhibitor of the mitochondrial Ca²⁺ uniporter (40, 41) in mammals (42–44). After accumulation of Ca²⁺ and addition of RR, Ca²⁺ efflux could be stimulated by Na⁺ (Fig. 2A, traces *c–e*) in the range 0.1–10 mM, with a concentration dependence (Fig. 2B) that is very similar to the Na⁺-Ca²⁺ antiporter of mammalian mitochondria (45–48), recently identified as NCLX (49).

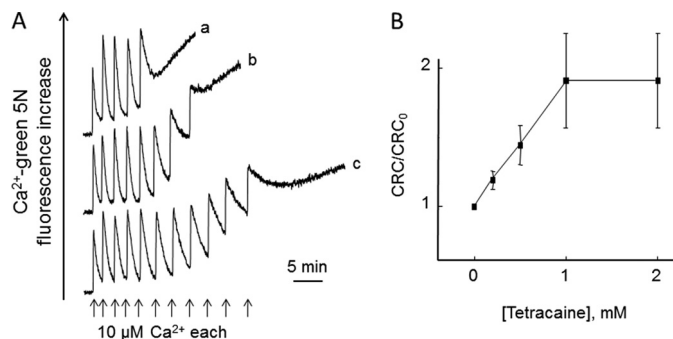


FIGURE 3. Effect of tetracaine on CRC of permeabilized *Drosophila* S₂R⁺ cells. Experimental conditions were as described in the legend to Fig. 2, except that the concentration of P_i was 1 mM. *A*, extramitochondrial Ca²⁺ was monitored, and CRC was determined by stepwise addition of 10 μM Ca²⁺ pulses (arrows) in the absence of further additions (trace *a*) or in the presence of 0.5 or 1 mM tetracaine (traces *b* and *c*, respectively). *B*, The amount of Ca²⁺ accumulated prior to onset of Ca²⁺-induced Ca²⁺ release in presence of the stated concentrations of tetracaine was normalized to that obtained in absence of tetracaine (CRC₀).

Addition of RR alone after Ca²⁺ uptake was followed by a slow process of Ca²⁺ release (Fig. 2C, trace *b*), which suggests the existence of a Na⁺-insensitive Ca²⁺ release pathway as also found in mammalian mitochondria (10). Addition of FCCP after accumulation of Ca²⁺ caused a fast process of Ca²⁺ release (Fig. 2C, trace *c*), which was only partly inhibited by RR (Fig. 2C, trace *d*) without any additional inhibitory effect of cyclosporin A (Fig. 2C, trace *e*). These experiments suggest the presence of a voltage-dependent Ca²⁺ release pathway (the RR-insensitive fraction of FCCP-induced Ca²⁺ release) resembling the PTP of mammalian mitochondria except for its lack of sensitivity to cyclosporin A (50, 51). We screened additional compounds for potential inhibition of RR-insensitive, FCCP-induced Ca²⁺ release, and we found a concentration-dependent inhibition by tetracaine (Fig. 2D, traces *b–d*), which also inhibits the PTP of mammalian mitochondria (52, 53).

We next studied the Ca²⁺ retention capacity (CRC) of *Drosophila* mitochondria by adding a train of Ca²⁺ pulses to permeabilized cells (Fig. 3). Ca²⁺ uptake was followed by spontaneous Ca²⁺ release (Fig. 3A, trace *a*), which was accompanied by mitochondrial depolarization (results not shown) and delayed by tetracaine (Fig. 3A, traces *b* and *c*), which considerably increased the CRC (Fig. 3B). Note that the rate of Ca²⁺ uptake was not affected by tetracaine, indicating that the Ca²⁺ uniporter is not inhibited by this drug.

The CRC was strikingly affected by P_i, in the sense that the threshold Ca²⁺ load required for onset of Ca²⁺ release increased at increasing concentrations of P_i (Fig. 4). The rate of spontaneous Ca²⁺ release decreased at increased P_i concentrations despite the larger matrix Ca²⁺ load (Fig. 4A). The half-maximal effect of P_i was seen at ~1 mM, which is similar to that required for inhibition by P_i of the PTP of yeast (23, 54) and of the PTP of mammals in cyclophilin D null mitochondria and in wild-type mitochondria treated with cyclosporin A (30).

We also tested the effect on the CRC of Ub0, a cyclophilin D-independent inhibitor of the mammalian pore (55, 56) and of the combination of ADP plus oligomycin, which is very effective at desensitizing the PTP to Ca²⁺ (57). No changes of CRC were observed with any of these PTP inhibitors, irrespective of whether the P_i concentration was 1 or 5 mM (supplemental Fig. 2).

Mitochondrial Ca^{2+} -induced Ca^{2+} release could be induced by the dithiol oxidant diamide (Fig. 5A) in a process that was prevented by dithiothreitol (Fig. 5B). Ca^{2+} release could also be induced by *N*-ethylmaleimide (NEM) (Fig. 6) after a lag phase that decreased as the concentration of NEM was increased (Fig. 6B) in the same range causing PTP opening in mammalian mitochondria (58).

We assessed mitochondrial volume changes in mitochondria subjected to an appropriate Ca^{2+} load sufficient to cause spon-

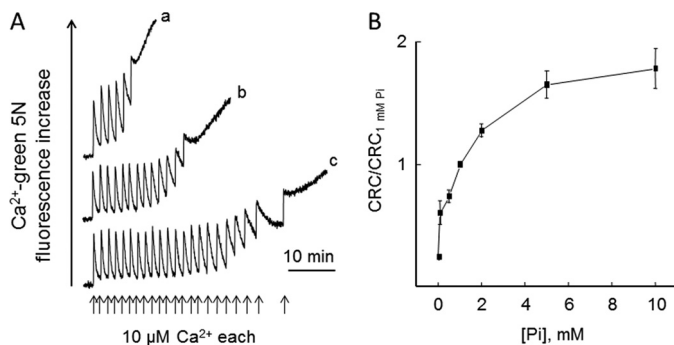


FIGURE 4. Effect of P_i on CRC of permeabilized *Drosophila* S_2R^+ cells. Experimental conditions were as described in the legend to Fig. 2, except that the concentration of P_i in A was 0.1, 1, or 5 mM (traces a, b, and c, respectively) or as indicated on the abscissa in B, where the CRC was normalized to the one obtained in the presence of 1 mM P_i ($\text{CRC}_{1 \text{ mM } \text{P}_i}$).

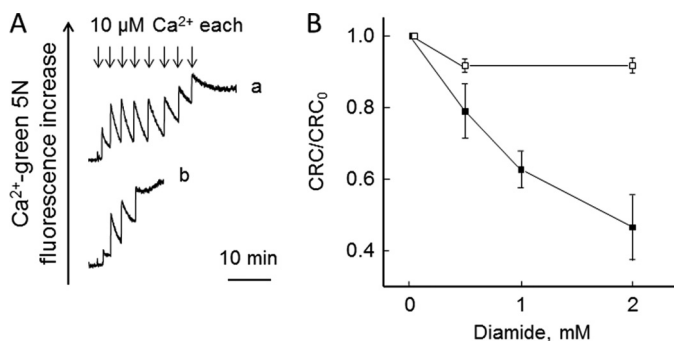


FIGURE 5. Effect of diamide on CRC of permeabilized *Drosophila* S_2R^+ cells. Experimental conditions were as in Fig. 2, except that the concentration of P_i was 1 mM. A, where indicated, 10 μM Ca^{2+} pulses (arrows) were added in the absence (trace a) or presence of 2 mM diamide (trace b). B, the CRC in presence of the stated concentrations of diamide alone (closed symbols) or after treatment with 1 mM dithiothreitol 1 min after diamide (open symbols) was normalized to that obtained in absence of diamide (CRC_0).

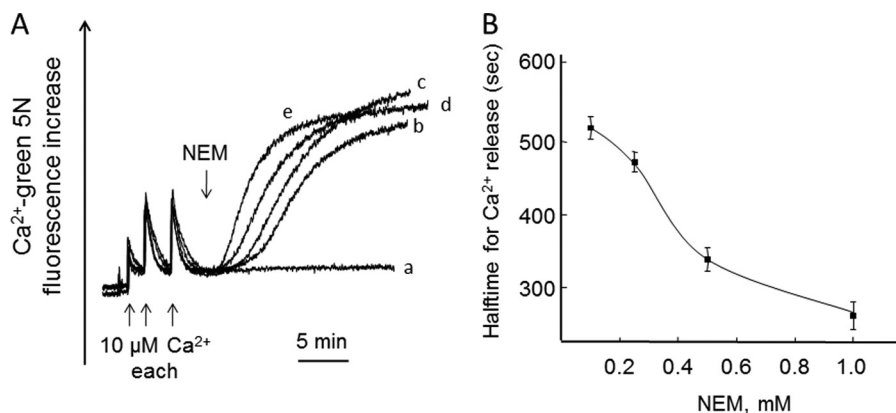


FIGURE 6. Effect of NEM on Ca^{2+} retention of permeabilized *Drosophila* S_2R^+ cells. Experimental conditions were as in Fig. 5. A, three 10 μM Ca^{2+} pulses were added followed by 0.05 (trace a), 0.1 (trace b), 0.25 (trace c), 0.5 (trace d), or 1 mM NEM (trace e). B, half-time required for Ca^{2+} release was calculated for experiments like those depicted in A.

aneous Ca^{2+} release at 0.1 mM P_i . Parallel readings of Ca^{2+} fluxes (Fig. 7A) and of light scattering at 540 nm (a sensitive measure of mitochondrial volume changes, Fig. 7B) revealed that after the small light scattering increase (matrix volume contraction) accompanying Ca^{2+} uptake no matrix swelling (which should manifest itself as a decreased light scattering) could be detected after the onset of Ca^{2+} release (Fig. 7B). It should be noted that mitochondria in permeabilized S_2R^+ cells can undergo swelling upon addition of the pore-forming peptide alamethicin, which also caused rapid release of residual matrix Ca^{2+} (Fig. 7), or of the selective K^+ ionophore valinomycin (supplemental Fig. 3). Mitochondrial Ca^{2+} -dependent Ca^{2+} release was not accompanied by cytochrome *c* release, which was instead readily elicited by the addition of alamethicin (Fig. 7C). This result is particularly striking because our experiments were carried out in KCl-based medium, which promotes ready cytochrome *c* removal if the outer membrane breaks following osmotic swelling of mammalian mitochondria (59). Electron microscopy fully confirmed that the condensed mitochondrial morphology was totally unaffected by a load of Ca^{2+} able to induce full Ca^{2+} release (compare the left and middle panels of Fig. 7D). This is a unique feature compared with the swelling response of mitochondria from all sources tested so far under similar conditions (19). On the other hand, mitochondrial swelling was readily detected after the addition of alamethicin (Fig. 7D, right panel).

DISCUSSION

In this work, we have characterized the pathways for Ca^{2+} transport in mitochondria from digitonin-permeabilized *Drosophila* S_2R^+ cells. These cells were originally derived from late embryonic stages (20–24 h), and selection was made based on the ability to adhere to tissue culture dishes (60). According to Schneider (60), they represent a variety of tissue precursors, and we assume that they are representative of *Drosophila*, although a full characterization of the Ca^{2+} release channel will have to await its molecular definition.

We have found that mitochondria of S_2R^+ cells possess the classical pathways found in mammalian mitochondria, *i.e.* (i) the RR-sensitive Ca^{2+} uniporter, which has been characterized by electrophysiology (12) and recently identified at the molecular level in mammals (40, 41). The existence in the *Drosophila*

Mitochondrial Ca²⁺ Transport in *Drosophila*

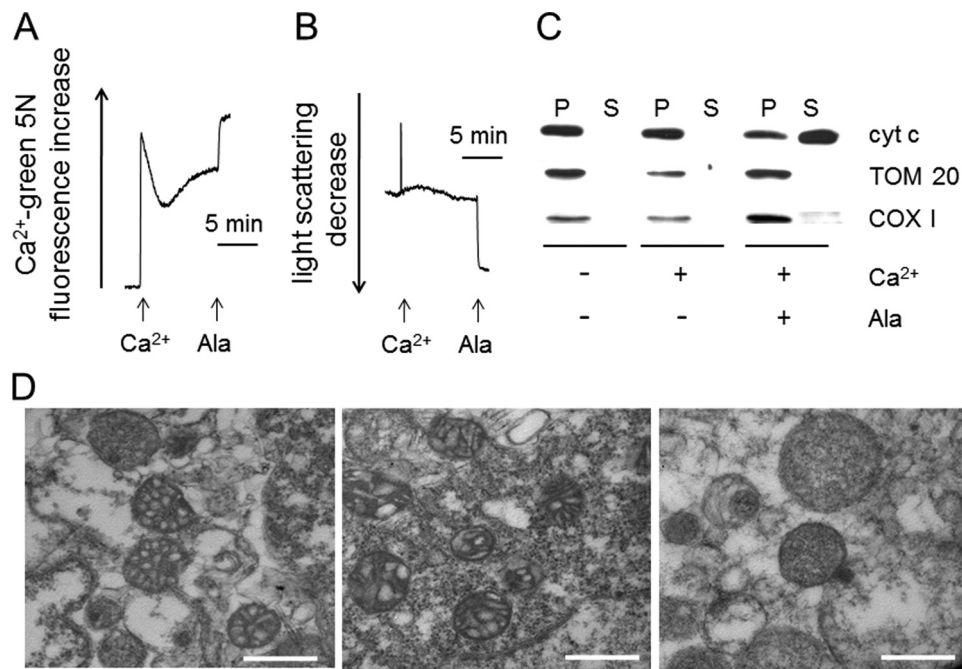


FIGURE 7. Effect of Ca²⁺ on light scattering, release of cytochrome c and mitochondrial ultrastructure in permeabilized *Drosophila* S₂R⁺ cells. Experimental conditions were as described in the legend to Fig. 2, except that the concentration of P_i was 0.1 mM and calcium Green 5N was omitted in the experiments of B. A and B, where indicated, 40 μM Ca²⁺ and 3 μM alamethicin were added. C, permeabilized cells were centrifuged before the addition of Ca²⁺, after addition of 40 μM Ca²⁺ or after addition of 40 μM Ca²⁺ and 3 μM alamethicin (as indicated by + and – symbols); pellets (P) and supernatants (S) were subjected to SDS-PAGE, transfer, and subsequent Western blotting with specific antibodies against cytochrome (cyt) c, TOM 20, and cytochrome oxidase (COX) subunit I. D, permeabilized cells were fixed and processed for electron microscopy before the addition of Ca²⁺ (left panel), after addition of 40 μM Ca²⁺ (middle panel) or after addition of 40 μM Ca²⁺ and 3 μM alamethicin (right panel); bar, 200 nm.

genome of close orthologs of the mitochondrial Ca²⁺ uniporter (40, 41) and of the previously identified MICU1 (61) (CG18769 and CG4495, respectively) predicts the existence of a mitochondrial Ca²⁺ uniporter in keeping with our findings. (ii) The Na⁺-Ca²⁺ antiporter recently identified as NCLX (49), whose ortholog also exists in *Drosophila* (CG14744) and is the likely mediator of the Na⁺-dependent Ca²⁺ release defined here. (iii) The putative H⁺-Ca²⁺ antiporter mediating Ca²⁺ release at high membrane potential, which can be unmasked by the addition of RR (10). Notably, it recently has been proposed that LETM1 (and its *Drosophila* ortholog CG4589) mediates H⁺-Ca²⁺ exchange by catalyzing RR-sensitive Ca²⁺ uptake in mitochondria (62). However, this contrasts with the well established role of LETM1 as a K⁺-H⁺ antiporter (63–66) and with the fact, confirmed here, that the putative H⁺-Ca²⁺ antiporter is insensitive to RR. (iv) A tetracaine-sensitive, RR-insensitive release pathway that opens in response to matrix Ca²⁺ loading or to depolarization and mediates Ca²⁺ release. The tetracaine-sensitive pathway, which displays unique features that appear to be intermediate between those of the PTP of yeast and mammals (31), is the main focus of the present manuscript.

Disequilibrium between Distribution of Ca²⁺ and Its Electrochemical Gradient—Ca²⁺ uptake is an electrophoretic process driven by the Ca²⁺ electrochemical gradient, $\Delta\bar{\mu}\text{Ca}$.

$$\Delta\bar{\mu}\text{Ca} = zF\Delta\psi + RT\ln[\text{Ca}^{2+}]_i/[\text{Ca}^{2+}]_o \quad (\text{Eq. 1})$$

In respiring mitochondria, the inside-negative $\Delta\psi$ favors uptake of Ca²⁺ (67, 68); and with a $\Delta\psi$ of –180 mV, the Ca²⁺ accumulation ratio at equilibrium (*i.e.* at $\Delta\bar{\mu}\text{Ca} = 0$) should be 10⁶ (69). This is never reached because at resting cytosolic Ca²⁺

levels, the rate of Ca²⁺ uptake is comparable with that of the efflux pathways, and Ca²⁺ distribution is governed by a kinetic steady state rather than by the thermodynamic equilibrium (69, 70). The activity of the mitochondrial Ca²⁺ uniporter and of the antiporters indeed creates a Ca²⁺ cycle across the inner membrane, whose energy requirement is very low (71) because the combined maximal rate of the efflux pathways is ~20 nmol Ca²⁺ × mg⁻¹ protein × min⁻¹ (10). On the other hand, because the V_{max} of the uniporter is ~1400 nmol Ca²⁺ × mg⁻¹ protein × min⁻¹, and its activity increases sharply with the increase of extramitochondrial [Ca²⁺] (72), this arrangement exposes mitochondria to the hazards of Ca²⁺ overload when cytosolic [Ca²⁺] increases. We have argued that the PTP may serve the purpose of providing mitochondria with a fast Ca²⁺ release channel (10, 14). This hypothesis is consistent with the effects of cyclosporin A on Ca²⁺ distribution in rat ventricular cardiomyocytes (73), with a PTP activating response to the combined action of two physiological stimuli increasing cytosolic [Ca²⁺] without detrimental effects on cell survival (17), and with the demonstration that cyclophilin D ablation causes mitochondrial Ca²⁺ overload *in vivo*, which, in turn, increases the propensity to heart failure after transaortic constriction, overexpression of Ca²⁺/calmodulin-dependent protein kinase IIδc or swimming exercise (16; see Ref. 75 for discussion).

Properties of *Drosophila* Ca²⁺-induced Ca²⁺ Release—The properties of the *Drosophila* Ca²⁺ release system described here appear to be intermediate between those of the PTP of mammals and yeast. Like the mammalian pore, *Drosophila* Ca²⁺ release is inhibited by tetracaine (52) and opens in response to matrix Ca²⁺ loading (76), inner membrane depo-

larization (77), thiol oxidation (78), and treatment with relatively high concentrations of NEM (58); like the yeast PTP (and at variance from the mammalian pore), it is inhibited by P_i (22, 23) and insensitive to cyclosporin A (23). The latter observations may be strictly related. P_i is a classical inducer of the mammalian PTP, yet P_i is essential for PTP inhibition by cyclosporin A and cyclophilin D ablation (30), suggesting that cyclophilin D masks an inhibitory site for P_i (79). It is interesting to note that a *Drosophila* mitochondrial cyclophilin has not been found and that even *Drosophila* Cyp1-PA, which according to the primary sequence, has a high probability of import into mitochondria, could not be found in the organelle after tagging with GFP and expression in S₂R⁺ and KC cells.⁴ It is tempting to speculate that lack of mitochondrial cyclophilin leaves the P_i inhibitory site unhindered and that the PTP-stimulating ability of P_i has developed after the evolutionary divergence of *Drosophila* and vertebrates.

At the onset of Ca²⁺-dependent Ca²⁺ release, *Drosophila* mitochondria undergo depolarization, suggesting that the putative channel is also permeable to H⁺. On the other hand, no matrix swelling is observed in KCl-based medium, indicating that the channel is not permeable to K⁺ (and Cl⁻), despite the fact that the hydrated radius of Ca²⁺ is larger than that of K⁺. Lack of swelling, which was confirmed by lack of cytochrome *c* release and by ultrastructural analysis, is not due to peculiar features of *Drosophila* mitochondria because matrix swelling and cytochrome *c* release readily followed the addition of the K⁺ ionophore valinomycin or of the pore-forming peptide alamethicin. We conclude that the putative Ca²⁺ release channel of *Drosophila* mitochondria is also permeable to H⁺. This is an essential feature because the Ca²⁺ diffusion potential created by efflux through a Ca²⁺-selective channel would otherwise oppose Ca²⁺ release (10).

Mitochondrial Ca²⁺-dependent Ca²⁺ Release as Mediator of Cell Death in Drosophila?—Available evidence points to persistent activation of the PTP as a prime mediator of apoptotic or necrotic cell death in a variety of situations (19). Indeed, unregulated opening of the PTP and ensuing mitochondrial and cellular dysfunction may be responsible for the pathology that characterizes a variety of human diseases (19). Although many of the proteins important for apoptosis in mammalian cells are conserved in *Drosophila*, the role that mitochondria play in cell death in this organism remains controversial (74, 80). The apparent absence of a regulatory role for a mitochondrial cyclophilin in the function of the “*Drosophila* PTP” prevents an investigation based on the effects of cyclosporin A in cells. However, our functional studies pave the way for the application of the sophisticated genetic strategies available in *Drosophila* to define the molecular nature of the channel and its role in pathophysiology of Ca²⁺ homeostasis.

REFERENCES

- Friel, D. D. (2000) *Cell Calcium* **28**, 307–316
- Giacomello, M., Drago, I., Pizzo, P., and Pozzan, T. (2007) *Cell Death Differ.* **14**, 1267–1274
- Csordás, G., and Hajnóczky, G. (2009) *Biochim. Biophys. Acta* **1787**, 1352–1362
- Rizzuto, R., Marchi, S., Bonora, M., Aguiari, P., Bononi, A., De Stefani, D., Giorgi, C., Leo, S., Rimessi, A., Siviero, R., Zecchini, E., and Pinton, P. (2009) *Biochim. Biophys. Acta* **1787**, 1342–1351
- Kann, O., and Kovács, R. (2007) *Am. J. Physiol. Cell Physiol.* **292**, C641–657
- Nicholls, D. G. (2009) *Biochim. Biophys. Acta* **1787**, 1416–1424
- Rizzuto, R., Bernardi, P., and Pozzan, T. (2000) *J. Physiol. Lond.* **529**, 37–47
- Rizzuto, R., and Pozzan, T. (2003) *Nat. Genet.* **34**, 135–141
- Szabadkai, G., and Duchen, M. R. (2008) *Physiology* **23**, 84–94
- Bernardi, P. (1999) *Physiol. Rev.* **79**, 1127–1155
- Gunter, T. E., and Gunter, K. K. (2001) *IUBMB Life* **52**, 197–204
- Kirichok, Y., Krapivinsky, G., and Clapham, D. E. (2004) *Nature* **427**, 360–364
- Gunter, T. E., and Sheu, S. S. (2009) *Biochim. Biophys. Acta* **1787**, 1291–1308
- Bernardi, P., and Petronilli, V. (1996) *J. Bioenerg. Biomembr.* **28**, 131–138
- Ichas, F., Jouaville, L. S., and Mazat, J. P. (1997) *Cell* **89**, 1145–1153
- Elrod, J. W., Wong, R., Mishra, S., Vagnozzi, R. J., Sakthivel, B., Goonasekera, S. A., Karch, J., Gabel, S., Farber, J., Force, T., Brown, J. H., Murphy, E., and Molkentin, J. D. (2010) *J. Clin. Invest.* **120**, 3680–3687
- Barsukova, A., Komarov, A., Hajnóczky, G., Bernardi, P., Bourdette, D., and Forte, M. (2011) *Eur. J. Neurosci.* **33**, 831–842
- Rasola, A., Sciacovelli, M., Pantic, B., and Bernardi, P. (2010) *FEBS Lett.* **584**, 1989–1996
- Bernardi, P., Krauskopf, A., Basso, E., Petronilli, V., Blachly-Dyson, E., Di Lisa, F., and Forte, M. A. (2006) *FEBS J.* **273**, 2077–2099
- Prieto, S., Bouillaud, F., Ricquier, D., and Rial, E. (1992) *Eur. J. Biochem.* **208**, 487–491
- Guérin, B., Bunoust, O., Rouqueys, V., and Rigoulet, M. (1994) *J. Biol. Chem.* **269**, 25406–25410
- Prieto, S., Bouillaud, F., and Rial, E. (1996) *Arch. Biochem. Biophys.* **334**, 43–49
- Jung, D. W., Bradshaw, P. C., and Pfeiffer, D. R. (1997) *J. Biol. Chem.* **272**, 21104–21112
- Roucou, X., Manon, S., and Guérin, M. (1997) *Biochim. Biophys. Acta* **1324**, 120–132
- Uribe-Carvajal, S., Luévano-Martínez, L. A., Guerrero-Castillo, S., Cabrera-Orefice, A., Corona-de-la-Peña, N. A., and Gutiérrez-Aguilar, M. (2011) *Mitochondrion* **11**, 382–390
- Fournier, N., Ducet, G., and Crevat, A. (1987) *J. Bioenerg. Biomembr.* **19**, 297–303
- Crompton, M., Ellinger, H., and Costi, A. (1988) *Biochem. J.* **255**, 357–360
- Broekemeier, K. M., Kloeck, C. K., and Pfeiffer, D. R. (1998) *Biochemistry* **37**, 13059–13065
- Halestrap, A. P., and Davidson, A. M. (1990) *Biochem. J.* **268**, 153–160
- Basso, E., Petronilli, V., Forte, M. A., and Bernardi, P. (2008) *J. Biol. Chem.* **283**, 26307–26311
- Azzolin, L., von Stockum, S., Basso, E., Petronilli, V., Forte, M. A., and Bernardi, P. (2010) *FEBS Lett.* **584**, 2504–2509
- Manon, S., Roucou, X., Guérin, M., Rigoulet, M., and Guérin, B. (1998) *J. Bioenerg. Biomembr.* **30**, 419–429
- Yanagawa, S., Lee, J. S., and Ishimoto, A. (1998) *J. Biol. Chem.* **273**, 32353–32359
- Bernardi, P., Scorrano, L., Colonna, R., Petronilli, V., and Di Lisa, F. (1999) *Eur. J. Biochem.* **264**, 687–701
- Taupin, P. (2008) *Eur. J. Histochem.* **52**, 135–139
- Angelin, A., Tiepolo, T., Sabatelli, P., Grumati, P., Bergamin, N., Golfieri, C., Mattioli, E., Gualandi, F., Ferlini, A., Merlini, L., Maraldi, N. M., Bonaldo, P., and Bernardi, P. (2007) *Proc. Natl. Acad. Sci. U.S.A.* **104**, 991–996
- Chiara, F., Castellaro, D., Marin, O., Petronilli, V., Brusilow, W. S., Juhaszova, M., Sollott, S. J., Forte, M., Bernardi, P., and Rasola, A. (2008) *PLoS One* **3**, e1852
- Azzolin, L., Basso, E., Argenton, F., and Bernardi, P. (2010) *Biochim. Biophys. Acta* **1797**, 1775–1779
- Hackenbrock, C. R. (1966) *J. Cell Biol.* **30**, 269–297
- De Stefani, D., Raffaello, A., Teardo, E., Szabó, I., and Rizzuto, R. (2011) *Nature* **476**, 336–340

⁴ K. R. Jones and M. A. Forte, unpublished results.

41. Baughman, J. M., Perocchi, F., Girgis, H. S., Plovanich, M., Belcher-Timme, C. A., Sancak, Y., Bao, X. R., Strittmatter, L., Goldberger, O., Bogorad, R. L., Kotliansky, V., and Mootha, V. K. (2011) *Nature* **476**, 341–345
42. Moore, C. L. (1971) *Biochem. Biophys. Res. Commun.* **42**, 298–305
43. Carafoli, E., and Sacktor, B. (1972) *Biochem. Biophys. Res. Commun.* **49**, 1498–1503
44. Vasington, F. D., Gazzotti, P., Tiozzo, R., and Carafoli, E. (1972) *Biochim. Biophys. Acta* **256**, 43–54
45. Carafoli, E., Tiozzo, R., Lugli, G., Crovetto, F., and Kratzing, C. (1974) *J. Mol. Cell Cardiol.* **6**, 361–371
46. Crompton, M., Capano, M., and Carafoli, E. (1976) *Eur. J. Biochem.* **69**, 453–462
47. Crompton, M., Künzi, M., and Carafoli, E. (1977) *Eur. J. Biochem.* **79**, 549–558
48. Crompton, M., Moser, R., Lüdi, H., and Carafoli, E. (1978) *Eur. J. Biochem.* **82**, 25–31
49. Palty, R., Silverman, W. F., Hershfinkel, M., Caporale, T., Sensi, S. L., Parnis, J., Nolte, C., Fishman, D., Shoshan-Barmatz, V., Herrmann, S., Khananshvil, D., and Sekler, I. (2010) *Proc. Natl. Acad. Sci. U.S.A.* **107**, 436–441
50. Broekemeier, K. M., Dempsey, M. E., and Pfeiffer, D. R. (1989) *J. Biol. Chem.* **264**, 7826–7830
51. Petronilli, V., Cola, C., and Bernardi, P. (1993) *J. Biol. Chem.* **268**, 1011–1016
52. Dawson, A. P., Selwyn, M. J., and Fulton, D. V. (1979) *Nature* **277**, 484–486
53. Broekemeier, K. M., Schmid, P. C., Schmid, H. H., and Pfeiffer, D. R. (1985) *J. Biol. Chem.* **260**, 105–113
54. Yamada, A., Yamamoto, T., Yoshimura, Y., Gouda, S., Kawashima, S., Yamazaki, N., Yamashita, K., Kataoka, M., Nagata, T., Terada, H., Pfeiffer, D. R., and Shinohara, Y. (2009) *Biochim. Biophys. Acta* **1787**, 1486–1491
55. Cesura, A. M., Pinard, E., Schubanel, R., Goetschy, V., Friedlein, A., Langen, H., Polcic, P., Forte, M. A., Bernardi, P., and Kemp, J. A. (2003) *J. Biol. Chem.* **278**, 49812–49818
56. Krauskopf, A., Eriksson, O., Craigen, W. J., Forte, M. A., and Bernardi, P. (2006) *Biochim. Biophys. Acta* **1757**, 590–595
57. Novgorodov, S. A., Gudiz, T. I., Milgrom, Y. M., and Brierley, G. P. (1992) *J. Biol. Chem.* **267**, 16274–16282
58. Pfeiffer, D. R., Schmid, P. C., Beatrice, M. C., and Schmid, H. H. (1979) *J. Biol. Chem.* **254**, 11485–11494
59. Jacobs, E. E., and Sanadi, D. R. (1960) *J. Biol. Chem.* **235**, 531–534
60. Schneider, I. (1972) *J. Embryol. Exp. Morphol.* **27**, 353–365
61. Perocchi, F., Gohil, V. M., Girgis, H. S., Bao, X. R., McCombs, J. E., Palmer, A. E., and Mootha, V. K. (2010) *Nature* **467**, 291–296
62. Jiang, D., Zhao, L., and Clapham, D. E. (2009) *Science* **326**, 144–147
63. Nowikovsky, K., Froschauer, E. M., Zsurka, G., Samaj, J., Reipert, S., Kolisek, M., Wiesenberger, G., and Schweyen, R. J. (2004) *J. Biol. Chem.* **279**, 30307–30315
64. Nowikovsky, K., Reipert, S., Devenish, R. J., and Schweyen, R. J. (2007) *Cell Death Differ.* **14**, 1647–1656
65. Dimmer, K. S., Navoni, F., Casarin, A., Trevisson, E., Endeke, S., Winterpacht, A., Salviati, L., and Scorrano, L. (2008) *Hum. Mol. Genet.* **17**, 201–214
66. McQuibban, A. G., Joza, N., Meghian, A., Scorzeto, M., Zanini, D., Reipert, S., Richter, C., Schweyen, R. J., and Nowikovsky, K. (2010) *Hum. Mol. Genet.* **19**, 987–1000
67. Scarpa, A., and Azzone, G. F. (1970) *Eur. J. Biochem.* **12**, 328–335
68. Wingrove, D. E., Amatruda, J. M., and Gunter, T. E. (1984) *J. Biol. Chem.* **259**, 9390–9394
69. Azzone, G. F., Pozzan, T., Massari, S., Bragadin, M., and Dell'Antone, P. (1977) *FEBS Lett.* **78**, 21–24
70. Nicholls, D. G. (1978) *Biochem. J.* **176**, 463–474
71. Stucki, J. W., and Ineichen, E. A. (1974) *Eur. J. Biochem.* **48**, 365–375
72. Bragadin, M., Pozzan, T., and Azzone, G. F. (1979) *Biochemistry* **18**, 5972–5978
73. Altschuld, R. A., Hohl, C. M., Castillo, L. C., Garleb, A. A., Starling, R. C., and Brierley, G. P. (1992) *Am. J. Physiol.* **262**, H1699–1704
74. Wang, C., and Youle, R. J. (2009) *Annu. Rev. Genet.* **43**, 95–118
75. Di Lisa, F., Carpi, A., Giorgio, V., and Bernardi, P. (2011) *Biochim. Biophys. Acta* **1813**, 1316–1322
76. Hunter, D. R., Haworth, R. A., and Southard, J. H. (1976) *J. Biol. Chem.* **251**, 5069–5077
77. Bernardi, P. (1992) *J. Biol. Chem.* **267**, 8834–8839
78. Petronilli, V., Costantini, P., Scorrano, L., Colonna, R., Passamonti, S., and Bernardi, P. (1994) *J. Biol. Chem.* **269**, 16638–16642
79. Giorgio, V., Soriano, M. E., Basso, E., Bisetto, E., Lippe, G., Forte, M. A., and Bernardi, P. (2010) *Biochim. Biophys. Acta* **1797**, 1113–1118
80. Krieser, R. J., and White, K. (2009) *Apoptosis* **14**, 961–968